Grazer Schriften der Geographie und Raumforschung Band 45/2010 pp. 303 - 312

Satellite Derived Snow and Runoff Dynamics in the Upper Indus River Basin

W.W. Immerzeel[1,2], P. Droogers[1], S.M. de Jong[2] and M.F.P. Bierkens[2]
[1]FutureWater, Costerweg 1G, 6702 AA Wageningen, The Netherlands
[2]Utrecht University, Faculty of Geosciences, PO Box 80115, Utrecht, The Netherlands

Abstract

Various remote sensing products are used to identify spatial-temporal trends in snow cover in the upper Indus basin from 1999 to 2008. It is shown that remote sensing allows detection of spatial-temporal patterns of snow cover across large areas in inaccessible terrain, providing useful information on a critical component of the hydrological cycle. The upper Indus basin is, for its water resources, most dependent on snow and ice melt and large parts are snow covered for prolonged periods of the year. A significant negative winter snow cover trend was identified for the upper Indus basin. A hydrological model is used and forced with remotely sensed derived precipitation and snow cover. The model is calibrated using daily discharges from 2000 to 2005 and stream flow in the upper Indus basin can be predicted with a high degree of accuracy. From the analysis it is concluded that there are indications that climate change is affecting the hydrology of the upper Indus basin due to accelerated glacial melting. This conclusion is primarily based on the observation that the average annual precipitation over a five year period is less than the observed stream flow.

KEY WORDS: MODIS, TRMM, snow cover, runoff, climate change, upper Indus

1. Introduction

The Himalayas and the adjacent Tibetan-Qinghai plateau are the source of the major Asian rivers amongst which are the Indus, Ganges, Brahmaputra, Irrawaddy, Salween, Mekong, Yellow and Yangtze rivers. Discharge from these rivers sustains the lives of hundreds millions of people living downstream and preservation of these water resources is crucial (Immerzeel 2008a). The precipitation in the upstream parts of the basins falls partly in the form of snow, causing a natural delay of river discharge. Snow cover dynamics on the Eurasian plateau therefore influence the water availability downstream in the major river basins of Asia, specifically in spring at the onset of the (irrigation) growing season (Barnett et al. 2005; Immerzeel 2008b).

The recently published fourth assessment report of the International Panel on Climate Change (IPCC, 2007a) concludes that warming of the global climate system is unequivocal, as is now evident from observations of increases in global average air and ocean temperatures, widespread melting of snow and ice, and rising global average sea level. The IPCC (2007a) report also concludes that the warming is expected to be greatest over land and at most high northern latitudes, where snow cover is projected to contract, and that it is very likely that hot extremes, heat waves, and heavy precipitation events will continue to become more frequent. The spatial variation in observed and projected climate change is large and mountain ranges and their downstream areas are particularly vulnerable for several reasons. Firstly, the rate of warming in the lower troposphere increases with altitude, i.e. temperatures will increase more in high mountains than at low altitudes (Bradley et al. 2004). Secondly, mountain areas exhibit a large spatial variation in climate zones due to large differences in altitude over small horizontal distances. These conditions make mountain areas more vulnerable to climate change (Beniston et al. 1997). Finally, mountains play an important role in the water supply of downstream areas. More than one sixth of the global population depends on water supplied by mountains and changes in hydrology and water availability are expected to be large in mountain basins (Barnett et al. 2005; Viviroli et al. 2007). Especially the diminishing role of snow and ice as a natural store for water supply will have a tremendous impact.

For all of these reasons knowledge on snow cover dynamics and how it influences water availability is of great importance and surprisingly regional studies on this topic are largely lacking. The focus of this study is on the upper Indus basin, where snowmelt is a major determinant in water supply. First the spatial patterns of snow cover are explored in the basin using remote sensing. Using a calibrated snowmelt runoff model the relationship between air temperature, precipitation, snow cover and rain, snow and glacial runoff is then analyzed. The model is forced with different remote sensing data products.

2. Study area

The study area is the upper Indus basin upstream of the Tarbela dam (Fig. 1), which is a major dam and regulates water supply to the Indus irrigated areas together with the Mangla dam as part of the Indus Basin project. The total basin area is 200677 km^2 and the length of the river upstream the dam is approximately 1125 km. The upper Indus basin includes the Hunza, Gilgit, Shigar and Shyok sub-basins. The altitude of the basin ranges from 335 m to 8238 m (Fig. 2) and as a result, the climate within the basin varies greatly. The largest part of the basin (90%) is in the rain shadow of the Himalayas and not effected by the summer monsoon. Low intensity winter and spring precipitation originating from western low pressure systems are the primary source of water. A small part of the basin (10%) directly upstream of the Tarbela dam is unprotected by mountain ranges and subject to summer monsoon rainfall. Average annual precipitation is around 340 mm with a peak in February and in July. Stream flow is a combination of fast rain runoff in the lower part of the basin and slow snow and glacier runoff of the higher parts of the basin (Archer 2003; Ali and de Boer 2007). The melt water component is extremely important and the primary source for irrigation of the entire Indus basin.

3. Methodology

3.1. Datasets

Various datasets are used in this study and described below.

3.1.1. MODIS snow cover

The Moderate Resolution Imaging Spectroradiometer (MODIS) snow products are provided as a sequence of products beginning with a swath product, and progressing, through spatial and temporal transformations, to an 8-day global-gridded product. Given the extent of the study area the MOD10C2 product is used. The MOD10C2 is a climate modelling grid product at a 0.050 resolution with global coverage and 8-day availability. Pixel values depict the percentage of snow cover (Hall et al. 2002). For the period March 2000 to December 2006 the algorithm version 4 is used and from January 2007 to July 2008 version 5 of the algorithm is used.

Snow cover products derived from MODIS are based on a band rationing of MODIS band 4 (green) (0.545–0.565 µm) and band 6 (near-infrared) (1.628–1.652 µm). These bands

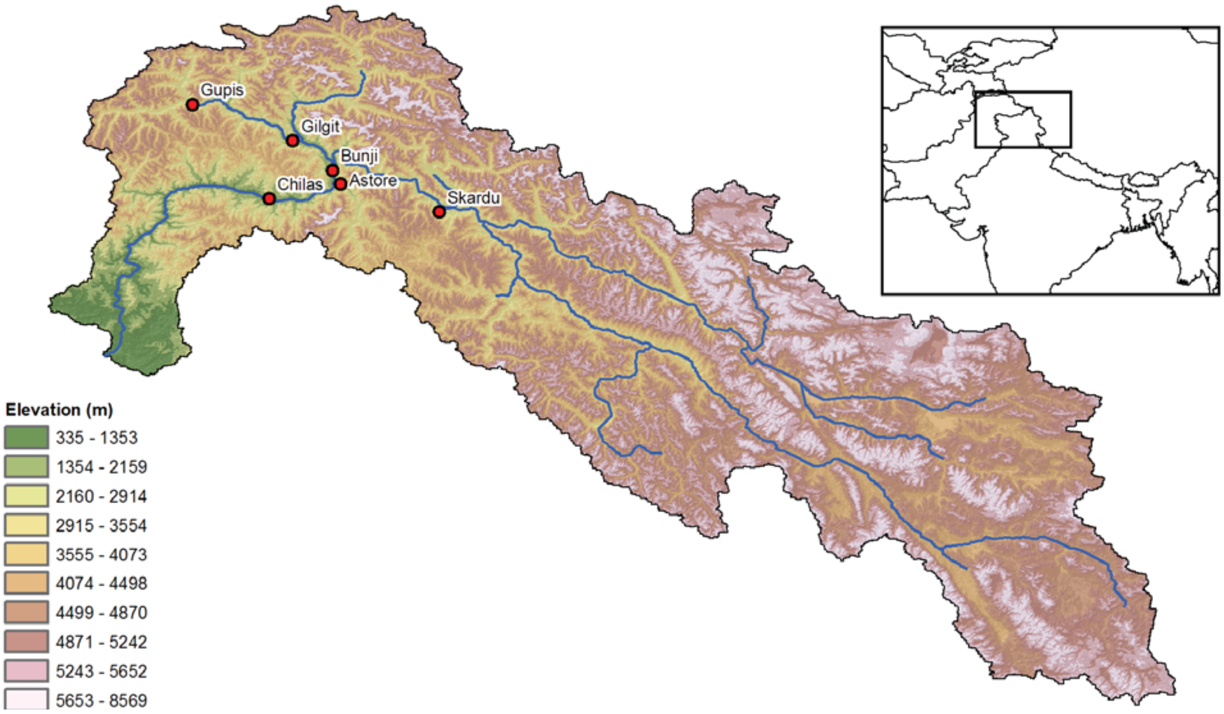

Figure 1: The location of the upper Indus basin, the elevation and the location of meteorological stations

are used to calculate the Normalized Difference Snow Index (NDSI) defined as

$$NDSI = \frac{band4 - band6}{band4 + band6}$$

In non-forested areas a pixel with an NDSI ffl 0.4 is identified as snow if the reflectance in band 2 (0.841–0.876 µm) ffl 11% and the reflectance in band 4 ffl 10%. (Hall et al. 1995). In forested areas an alternative algorithm is used that includes the Normalized Difference Vegetation Index (NDVI) (Klein et al. 1998). Using a threshold on the NDVI it is possible that a forested pixel is classified as snow even if the NDSI is lower than 0.4. The NDSI has been effectively used in snow cover mapping using various sensors (Dankers and de Jong 2004)

3.1.2. TRMM precipitation

The Tropical Rainfall Measuring Mission (TRMM) provides precipitation estimates at fine spatial scales using a calibration based sequential scheme and data from multiple satellites as well as gauge analysis. In this study the 3B43 product is used (Hufmann et al. 2007). This is a monthly product spanning a global belt from 500 N to 500 S with a spatial resolution of 0.250. The original processing occurs at a time interval of three hours. Firstly, a number of passive microwave sensors aboard TRMM and other satellites are converted to a precipitation estimate. Secondly, an infrared (IR) estimate is generated using the calibrated microwave estimate. Thirdly, the microwave and IR estimates are combined to provide the best estimate at each grid box at each three hour period. The final step in generating 3B43 is the inclusion of rain gauge data. It is highly advantageous to include rain gauge data in combination data sets. All 3-hourly combined microwave and IR estimates are then summed over a calendar month to create a monthly multi-satellite product. Using the gridded precipitation gauge based product of the Global Precipitation Climatological Centre (Rudolf 1993) a bias correction is performed in similar way as described in Hufmann et al. (1997).

3.1.3. Meteorological data

Daily meteorological data for six different stations in Pakistan from the Pakistan Meteorological Department were used to force the runoff model and to verify the TRMM data that were used. The location of the meteorological stations is shown in Fig. 1.

3.2. Runoff modelling

The runoff modelling in the upper Indus basin is based on the Snowmelt Runoff Model (SRM). The model was originally develop by Martinec (1975) and has been applied in over 100 basins ranging in surface area from 0.8 km² to 917444 km² in 29 different countries (Martinec et al. 2007) and results are published in about 80 scientific journals (Seidel and Martinec 2004). SRM is a conceptual, deterministic, degree day hydrologic model used to simulate daily runoff resulting from snowmelt and rainfall in mountainous regions. SRM requires daily temperature, precipitation and daily snow-covered area values as input parameters. Stream flow is calculated according to Eq. (1).

$$Q_{n+1} = [Cs_n \cdot a_n (T_n + \Delta T_n) S_n + Cr_n P_n] . A . (10000/86400) . (1-k_{n+1}) + Qn . k_{n+1} \quad (1)$$

Where Q_{n+1} (m^3/s) is the discharge at day n+1, Csn (-) is the snow runoff coefficient, a_n is the degree day factor on day n (cm °C^{-1} d^{-1}), $T_n + \Delta T_n$ (°C) are the degree days, S_n (-) is the fractional snow cover, Cr_n (-) is the rain runoff factor, P_n (cm) is the rain on day n, A is total area (km^2) and k_{n+1} is the discharge recession coefficient.

The original SRM model has been extended to model the effects of climate change and include glacial melt, which is an important component of total runoff in the upper Indus basin (Archer 2003). The glacier area is derived from the remotely sensed snow cover depletion curve by taking the 5% percentile value of the time series as a representative value of the permanent snow and ice cover. A glacial degree day factor is then used to calculate glacial melt similar to snow melt. To capture the spatial climate heterogeneity typical for mountain basins, the upper Indus basin has been stratified in three different elevation zones according to the area elevation curve (Fig. 2). The zonal reference elevations are 2000 m, 4700 m and 5000 m and the respective areas are 30497 km^2, 83778 km^2 and 86402 km^2. For each zone daily temperature data (T_n) are derived from a nearby meteorological station and temperatures are lapsed to the zonal reference elevation (ΔT_n). For each zone the model is forced with TRMM precipitation (3B43) which is disaggregated to daily values using precipitation gauge data and snow cover is derived using the MOD10C2 product. Eq. (1) is applied for each zone and the results are aggregated and provide the discharge at the outlet of the basin. The model is run from 2001 to 2005 and calibrated using daily discharge data at Besham Qila, a gauging station just upstream the Tarbela reservoir. The model is calibrated on a number of critical parameter such as the snow runoff coefficient (Cs_n), the rainfall runoff coefficient (Cr_n), the critical temperature below which precipitation falls in the form of snow (Tc) and the temperature lapse rate that is used to lapse the observed temperature to the zonal reference elevation (λ). Model results are assessed on the Pearson correlation coefficient, bias, root mean square error and the Nash Sutcliffe criterion.

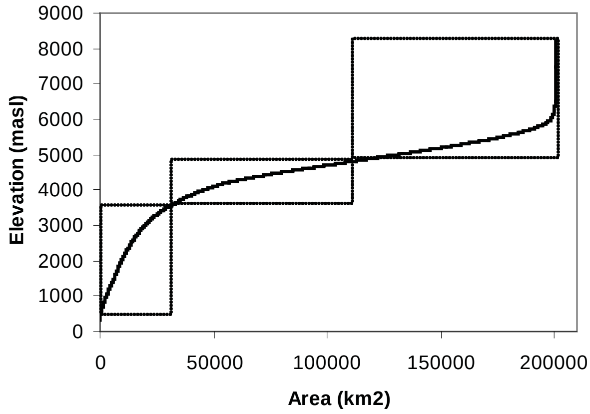

Figure 2: Area-elevation curve for the upper Indus basin. The dotted boxes show the elevation zones used in the runoff modelling. The reference elevation equals the median elevation of the elevation distribution within each box.

4. Results and discussion

4.1. Snow cover trends

The seasonal evolution of snow cover from 2000 to 2008 is shown in Fig. 3. The average annual snow cover for the upper Indus basin is high at 33.9% of the total area. Snow cover obviously is persistent in the upper Indus basin compared to other basins, and the snow cover peak is generally found during spring.

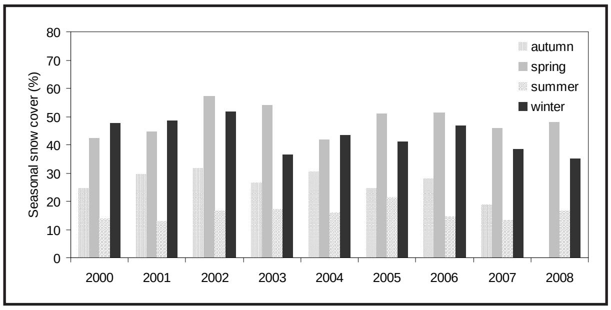

Figure 3: Seasonal snow cover from 2000 to 2008 based on MODIS MOD10C2 product for the upper Indus basin.

It was also investigated whether any seasonal trends could be observed in this dataset. The Pearson correlation coefficient was calculated for each season for the entire domain, for the upper Indus basin and for the three elevation zones in the basin. The significance of the correlations was tested at the 0.05 probability level assuming a t-distribution. Table 1 shows that a significant negative trend is found for winter snow cover in the upper Indus basin and in zone 2 (4700 m) and zone 3 (5000 m). The negative trend is strongest in zone 3 (2.2 % y^{-1}), followed by zone 2 (1.4 % y-1) and the entire basin (1.3 % y^{-1}). For all other seasons and areas no significant trends were identified. It should be noted though that the time series used for this analysis is relatively short (nine years), but it is currently the most reliable dataset available. Construction of a reliable long term snow cover record for this area would be highly recommendable.

	Upper Indus	Zone 1	Zone 2	Zone 3
spring	0.10	-0.13	-0.02	0.20
summer	0.22	0.17	0.22	0.21
autumn	-0.47	-0.44	-0.56	-0.16
winter	-0.68	0.29	-0.64	-0.78
annual	-0.30	-0.14	-0.47	-0.19

Table 1: Pearson correlation coefficients for seasonal trends in snow cover for the entire domain, the upper Indus basin and the three elevation zones. Bold numbers are significant at the 0.05 probability level.

Fig. 4 shows the seasonal extent and variation of snow cover in for the entire spatial domain. Values indicate the percentage of time that a pixel was snow covered during the indicated seasons within the entire time series from March 2000 to July 2008. There is an obvious relation with the elevation and especially in the upstream part of the upper Indus basin where there are large areas which are snow covered more than 90% of the time during winter and spring. The snow ablation peaks at the end of spring and in the beginning of summer, while winter precipitation provides new snow.

Using the Shuttle Radar Topographic Mission (SRTM) digital elevation model (Werner, 2001) in combination with the MOD10C2 time series seasonal snowline heights were determined. To avoid undesired effects of potential false classified snow pixels the snowline was defined as the 5% percentile of the elevation distribution of snow covered pixels in the basin. In the Indus basin the snow line varies from 2336 meter in winter to 3035 in spring to 3712 meter in autumn to 4109 meter in summer.

To what extent basin hydrology is really affected by snow and ice melt not only depends on snow cover patterns, but also on the temporal behaviour of precipitation. To quantify the relative importance of snow and ice melt to the annual stream flow the relative contribution of winter precipitation to spring precipitation and relative to total annual precipitation has been plotted in Fig. 5. The upstream part of the Indus basin receives most winter precipitation of the whole area. In combination with relative small amounts of precipitation during the summer the importance of snow and ice melt to total annual stream flow is much larger than in any other Himalayan basin. This becomes evident from the bottom two figures in Fig. 5. There are large areas in the Indus basins where winter precipitation is over 80 % of total spring precipitation and over 30 % of total annual precipitation. In the other basins these percentages are much lower and stream flow is mainly rain fed. From these results we conclude that stream flow in the Indus basin is for large part fed by snow

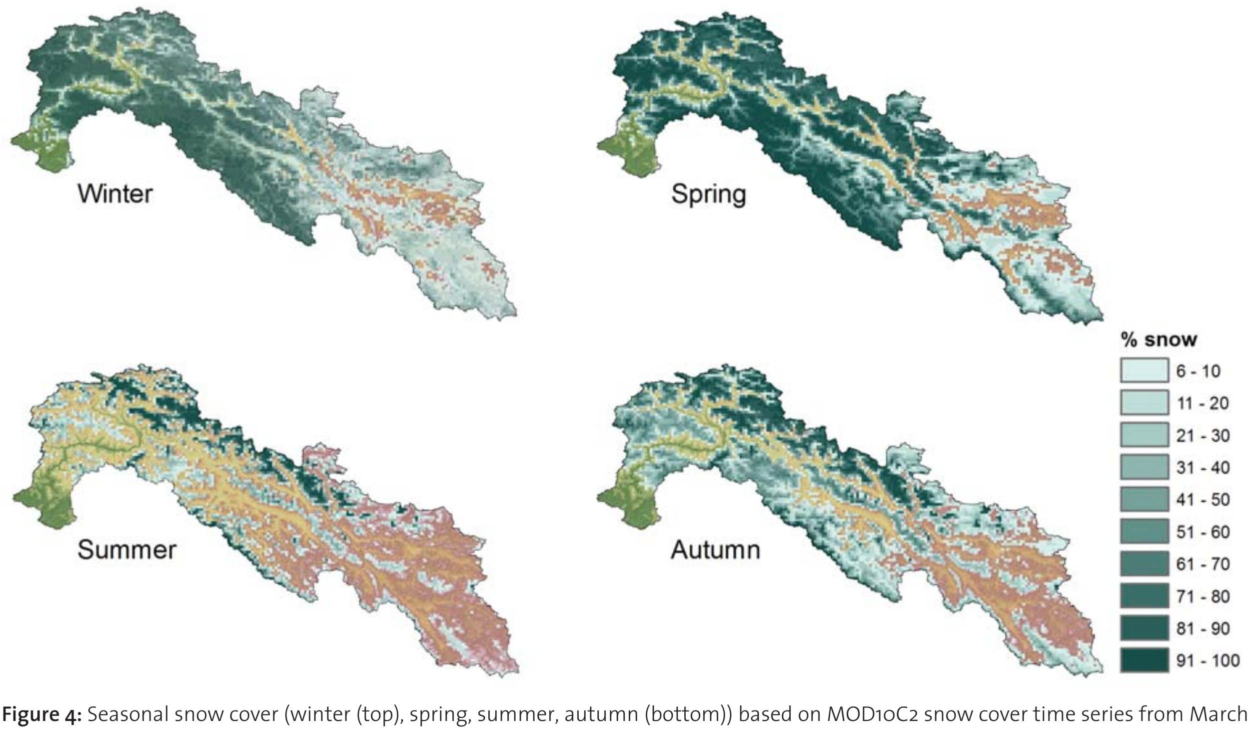

Figure 4: Seasonal snow cover (winter (top), spring, summer, autumn (bottom)) based on MOD10C2 snow cover time series from March 2000 to February 2008. The values show the percentage of time that a pixel was snow covered during the specified season within the entire time series.

and glacial melt in clear contrast to other Himalayan originating basins. This is further quantified by the snow and ice runoff modelling in the remainder of this paper.

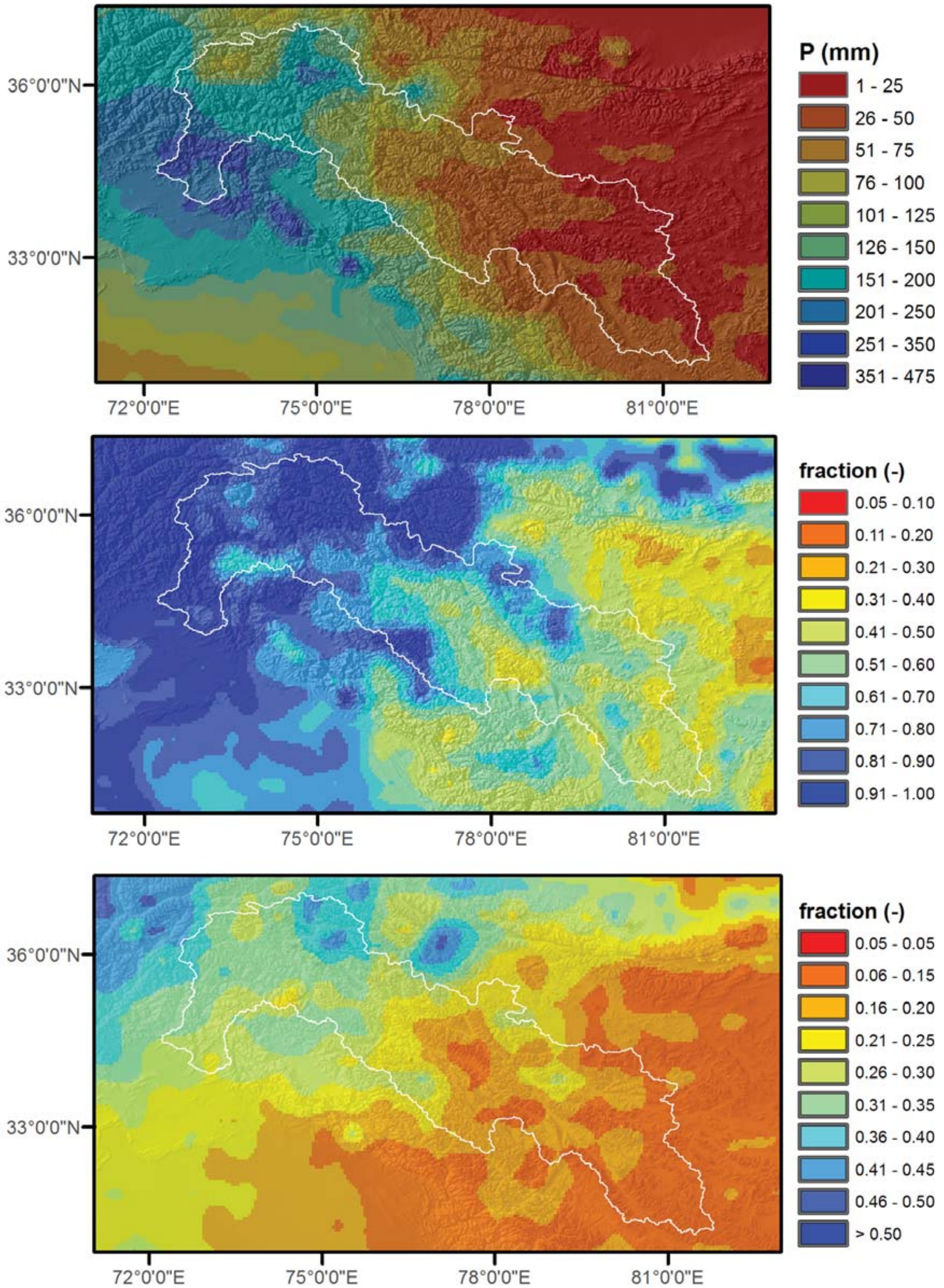

Figure 5: Sum of the average October to February (1998-2006) precipitation based on the TRMM 3B43 product (top figure), fraction of spring rainfall (middle figure) and fraction of annual rainfall (bottom figure).

4.2. Runoff modelling

An SRM based runoff model was set up for the upper Indus basin to improve the understanding of the contribution of snow melt, glacial melt and rain to total stream flow. The model is driven by remotely sensed snow cover and precipitation data. The model is calibrated on daily discharges from 2001 to 2005. Fig. 6 shows that the simulated stream flow matches the observed stream flow very well. Based on these time series a number of calibration assessment criteria were calculated. The Pearson correlation coefficient equalled 0.88, which is proof of an excellent correlation between observed and simulated daily stream flow. The bias is 0.02 which shows that the average observed stream flow is 2% higher than the simulated stream flow. The RMSE equals 1157 m^3/s, while the Nash-Sutcliffe criterion equals 0.78. From these criteria it is concluded that stream flow at Besham Qila is realistically simulated using the SRM based approach.

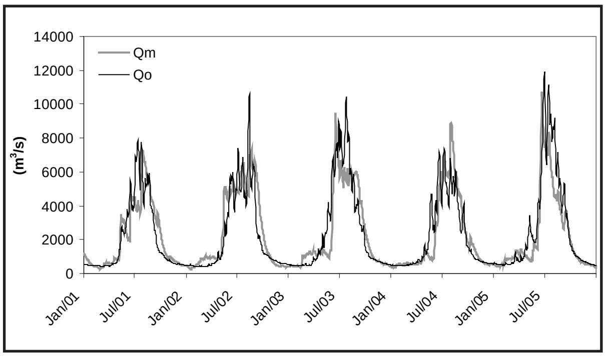

Figure 6: Modelled and observed daily stream flow at Besham Qila from 2001 to 2005.

Table 2 shows the average monthly model results for the period 2001-2005. The most striking feature of these results is the fact that the total TRMM 3B43 precipitation for the entire basin based equals 311 mm y^{-1}, while the total modelled stream flow at Besham Qila equals 359 mm y^{-1}. The modelled discharges match the observed discharge and it is concluded that there must be an additional source of water to explain the reported stream flow, especially considering that actual evapotranspiration is not accounted for. There are two possibilities. Firstly, precipitation is significantly underestimated, but this seams unlikely, because a recent study that assessed TRMM 3B43 satellite biases on the Tibetan plateau concluded that the TRMM 3B43 consistently overestimates observed precipitation (Yin et al. 2008). This would yield the opposite namely that the difference between basin precipitation and observed discharge would even be larger.

A second possible explanation is an increased glacial runoff due to global warming. The scientific literature is contradicting in this respect. Fowler and Archer (2006) report a thickening and expansion of Karakoram glaciers due to increased winter precipitation and decreasing summer temperatures. However, the IPCC reports that glaciers in the Himalaya are receding faster than in any other part of the world and that the receding and thinning of Himalayan glaciers can be attributed primarily to the global warming due to increase in anthropogenic emission of greenhouse gases (IPCC 2007b). The global land ice measurements from space (GLIMS) project also report a consistent decrease of glacier extent in the upper Indus basin in particular (Kargel et al. 2005). The findings of this study support the latter because we identify positive temperature trends in all seasons and an unexplained difference between basin precipitation and observed stream flow. Question remains if the additional source of water that is required to close the water balance can realistically be sustained by the ice reserves in the basin. If we assume that a minimum of 100 mm is required the volume of ice that is required approximately equals 22 km^3 of glacial ice with a density of 900 kg m^{-3}. A previous study revealed that the glacier coverage in the entire upper Indus basin is approximately 10% (Kulkarni et al. 2007). This is in good agreement with the value derived in this study using the 5% percentile of the MODIS based snow depletion curve (9.9 %). The average glacier thickness is reported to be around 100 meter (Kulkarni et al. 2007) and therefore the total ice reserve in the upper Indus basin is estimated to be 1982 km^3. Therefore it is concluded that 100 mm roughly equals 1% of the total ice reserve and is plausible. However more research is required to further substantiate these findings.

Fig. 7 shows that a large part of the precipitation indeed falls in the form of snow (60% on average). Figure 7 also reveals that on average 40% of the annual stream flow is generated by snow melt with a peak in June. Glacial melt contributes on average 32% with a peak in July and rain comprises 28% of total annual stream flow with a similar temporal pattern as glacial runoff. The majority of stream flow in the upper Indus (72%) is therefore a direct result of melting of snow and ice, and therefore highly susceptible to changes in temperature. The anticipated effects of climate changes are:

- Accelerated melt of glacier resulting in an increase in glacial runoff.
- Less precipitation will fall in the form of snow causing an increase in rain runoff on the expense of snow runoff.
- Snow will melt faster causing a shift in the hydrograph towards spring.

	P	r_q
January	12	5
February	32	9
March	28	13
April	30	13
May	23	33
June	33	90
July	51	85
August	43	63
September	32	26
October	13	8
November	6	6
December	9	6
Total	311	359

Table 2: Average monthly precipitation (p) and stream flow (q) from 2001-2005. All values are in mm.

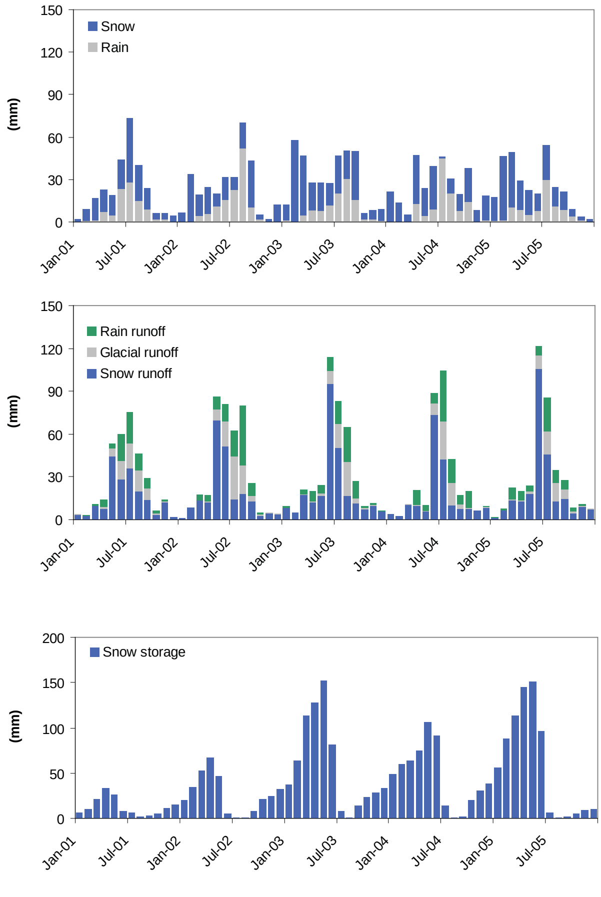

Figure 7: Monthly snow and rain (top), different runoff components (middle) and snow storage (bottom) from 2001 to 2005 for the upper Indus basin.

5. Conclusions

This study investigated the spatial and temporal coverage of snow and used a hydrological model to simulate rain, snow and glacial runoff in the upper Indus basin. A number of major conclusions can be drawn based on this study:

- Remote sensing allows detection of spatial-temporal patterns of snow cover across large areas in inaccessible terrain and provides useful information on a critical component of the hydrological cycle. Forcing a hydrological model with remotely sensed TRMM derived precipitation and MODIS based snow cover shows promising results and stream flow in the upper Indus basin can be predicted with a high degree of accuracy.
- The upper Indus basin is, for its water resources, highly dependent on snow and ice melt and large parts are snow covered for prolonged periods of the year. There is a significant negative snow cover trend found in winter in the upper Indus basins.
- There are indications that climate change is affecting the hydrology of the upper Indus basins due to the accelerated glacial melting. This conclusion is primarily based on the observation that the average annual precipitation over a five year period is less than the observed stream flow. The annual melting rate is conservatively estimated at 1% of the total ice reserve.

Acknowledgements

The authors are grateful to the Pakistan Meteorological Department for providing the meteorological data and to the Water and Power Development Authority for the discharge data.. This study was financially supported by the Netherlands Organisation for Scientific Research (NWO) through a CASIMIR grant (018 003 002).

References

ALI, K.J., DE BOER, D.H., 2007: Spatial patterns and variation of suspended sediment yield in the upper Indus River basin, northern Pakistan. Journal of Hydrology, 334, 368–387.

ARCHER, D., 2003: Contrasting hydrological regimes in the upper Indus Basin. Journal of Hydrology, 274, 198–210.

BARNETT T.P., ADAM J.C., LETTENMAIER D.P., 2005: Potential impacts of a warming climate on water availability in snow-dominated regions. Nature 438, 303-309, DOI 10.1038/nature04141

BENISTON M., DIAZ H.F., BRADLEY R.S., 1997: Climatic Change at high elevation sites: an overview. Climatic Change, 36, 233-251.

BRADLEY S.B., VUILLE M., DIAZ H.F., VERGARA W., 2006: Threats to water supplies in the tropical Andes. Science 312,1755-1756, DOI 10.1126/science.1128087

DANKERS R., DE JONG, S.M., 2004: Monitoring Snow Cover Dynamics in Northern Fennoscandia with SPOT VEGETATION Images. International Journal of Remote Sensing, 25, 2933-2949.

FOWLER, H.J., ARCHER, D.R., 2006: Conflicting Signals of Climatic Change in the Upper Indus Basin. J. Climate, 19, 4276–4293.

HALL, D. K., RIGGS, G. A., AND SALOMONSON, V. V., 1995: Development of methods for mapping global snow cover using Moderate Resolution Imaging Spectroradiometer (MODIS) data. Remote Sensing of Environment, 54, 127–140.

HALL D.K., RIGGS G.A., SALOMONSON V.V., DIGIROLAMO N.E., BAYR K.J., 2002: MODIS snow-cover products. Remote Sensing of Environment, 83, 181-194.

HUFFMAN, G. J., ADLER, R.F., ARKIN, P., CHANG, A., FERRARO, R., GRUBER, A., JANOWIAK, J., MCNAB, A., RUDOLF, B., SCHNEIDER, U., 1997: The global precipitation climatology project (GPCP) combined precipitation dataset, Bull. Amer. Meteor. Soc., 78, 5-20.

HUFFMAN, G.J., ADLER, R.F., BOLVIN, D.T., GU, G., NELKIN, E.J., BOWMAN, K.P., HONG, Y., STOCKER, E.F., WOLFF, D.B., 2007: The TRMM Multi-satellite Precipitation Analysis: Quasi-Global, Multi-Year, Combined-Sensor Precipitation Estimates at Fine Scale. J. Hydrometeor., 8(1), 38-55.

IMMERZEEL W.W., 2008a: Spatial modeling of mountainous basins: An integrated analysis of the hydrological cycle, climate change and agriculture. Netherlands Geographical Studies 369, KNAG, Utrecht.

IMMERZEEL, W.W., 2008b: Historical trends and future predictions of climate variability in the Brahmaputra basin. The International Journal of Climatology 28: 243:254.

IPCC, 2007a: Climate Change 2007: The Scientific Basis. Cambridge University Press, Cambridge.

IPCC, 2007b: Climate Change 2007: Impacts, Adaptation and Vulnerability. Cambridge University Press, Cambridge.

KARGEL, J. S., ABRAMS,M. J.,BISHOP, M. P., BUSH, A.,HAMILTON, G., JISKOOT,H., ET AL., 2005: Multispectral imaging contributions to global land ice measurements from space. Remote Sensing of Environment, 99, 187-219.

KLEIN, A. G., HALL, D. K., & RIGGS, G. A., 1998: Improving snow-cover mapping in forests through the use of a canopy reflectance model. Hydrological Processes, 12, 1723–1744.

KULKARNI, A.V., BAHUGUNA, I.M., RATHORE, B.P., SINGH, S.K., RANDHAWA, S.S., SOOD, R.K., DHAR S. , 2007: Glacial retreat in Himalaya using Indian Remote Sensing satellite data. Current Science 92: 69-74.

MARTINEC, J., 1975: Snowmelt-Runoff Model for stream flow forecasts. Nordic Hydrol. 6, 145-154.

MARTINEC, J., RANGO, A., ROBERTS, R., 2007: Snowmelt Runoff Model: User Manual. New Mexico State University, Las Cruces.

RUDOLF, B., 1993: Management and analysis of precipitation data on a routine basis. Proceedings of International Symposium on Precipitation and Evaporation, Vol. 1, B. Sevruk and M. Lapin, Eds., Slovak Hydrometeorology Institution, 69–76.

SEIDEL, K., MARTINEC, J., 2004: Remote Sensing in Snow Hydrology: Runoff Modelling, Effect of Climate Change. Springer.

VIVIROLI, D, DÜRR, HH, MESSERLI, B, MEYBECK, M, WEINGARTNER R., 2007: Mountains of the world, water towers for humanity: Typology, mapping, and global significance, Water Resources Research, 43, W07447, doi:10.1029/2006WR005653.

WERNER M., 2001: Shuttle Radar Topography Mission (SRTM), mission overview. Frequenz 55: 75–79.

YIN, Z-Y., ZHANG, X., LIU, X., COLELLA, M., CHEN, X., 2008: An Assessment of the Biases of Satellite Rainfall Estimates over the Tibetan Plateau and Correction Methods Based on Topographic Analysis. Journal of Hydrometeorology, 9, 301-326.

Correspondence to:

W.W. Immerzeel

FutureWater

Costerweg 1G, 6702 AA Wageningen, The Netherlands

e-mail: w.immerzeel@futurewater.nl

Utrecht University

Faculty of Geosciences

PO Box 80115, Utrecht, The Netherlands